Facile and Mild Strategy Toward Biopolymer-Coated Boron Nitride Nanotubes via a Glycine-Assisted Interfacial Process

ARTICLE *in* THE JOURNAL OF PHYSICAL CHEMISTRY C · AUGUST 2013

Impact Factor: 4.77 · DOI: 10.1021/jp4073729

6 AUTHORS, INCLUDING:

Yiu-Ting Richard Lau
Nano and Advanced Materials Institute
19 PUBLICATIONS **87** CITATIONS
SEE PROFILE

Xia Li
National Institute for Materials Science
45 PUBLICATIONS **778** CITATIONS
SEE PROFILE

Francoise Winnik
Université de Montréal
272 PUBLICATIONS **13,765** CITATIONS
SEE PROFILE

THE JOURNAL OF PHYSICAL CHEMISTRY C

Article

pubs.acs.org/JPCC

Facile and Mild Strategy Toward Biopolymer-Coated Boron Nitride Nanotubes via a Glycine-Assisted Interfacial Process

Yiu-Ting R. Lau,[†] Maho Yamaguchi,[†,‡] Xia Li,[†] Yoshio Bando,[†] Dmitri Golberg,*[,†,‡] and Françoise M. Winnik*[,†,§]

[†]World Premier International (WPI) Research Center Initiative, International Center for Materials Nanoarchitectonics (MANA) and National Institute for Materials Science (NIMS), 1-1 Namiki, Tsukuba 305-0044, Japan

[‡]Graduate School of Pure and Applied Science, University of Tsukuba, Tennodai 1-1-1, Tsukuba 3058577, Japan

[§]Faculté de Pharmacie and Département de Chimie, Université de Montréal, CP 6128 Succursale Centre Ville, Montreal, QC, H3C 3J7, Canada

Supporting Information

ABSTRACT: We report a simple way to obtain polymer-coated multiwalled boron nitride nanotubes (BNNTs) conducted under mild conditions compatible with fragile biopolymers. The approach converts aggregated pristine BNNTs into colloidally stable dispersions in water without requiring treatment at high temperature or in strongly oxidative conditions. The method relies on our experimental observation that glycine (NH_2-CH_2-COOH, Gly) interacts with BNNTs, in accordance with theoretical calculations. The role of glycine in this process is 2-fold: the Gly amine group binds to the B-sites of BNNTs, while the Gly carboxylic acid function provides ionic anchoring sites for interactions with polyelectrolytes. The formation of Gly-BNNTs proved to be essential, since they readily disperse in water as disentangled objects and spontaneously adsorb polycations, such as chitosan (CH), polyanions, such as hyaluronan (HA), and polyzwitterionic polymers, such as chitosan-phosphorylcholine (CH-PC). Treatment of aqueous dispersions of coarsely coated BNNTs with an immiscible solvent (hexane) resulted in the complete coverage of the BNNT surfaces via oil/water interfacial assembly. This work provides a rapid, mild, and scalable route to water-dispersible biofunctional BNNTs that may serve as drug delivery vehicles or scaffolds in tissue engineering.

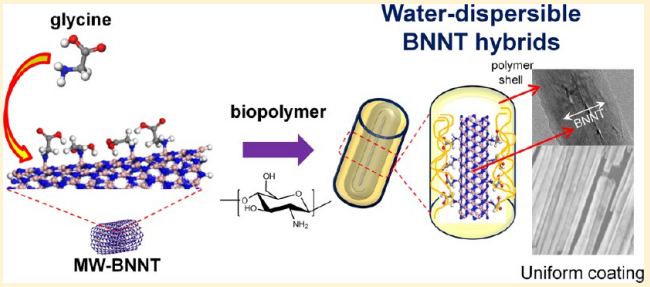

INTRODUCTION

Hybrid nanomaterials, which combine inorganic substances and synthetic or natural organic compounds, continue to attract much attention across diverse areas of materials science, as they elicit unique synergistic properties unattainable by traditional means.[1] Carbon nanotube (CNT) hybrids are among the most promising materials for future nanotechnologies, due to CNT outstanding physical and chemical properties. The CNT structural analogs - boron nitride nanotubes (BNNTs) - are not as widespread in today's materials science as their C counterparts. Their properties are very different from those of CNTs. BNNTs are wide band gap semiconductors (band gap ~5.5 eV) as opposed to the narrow band gap semiconducting or metallic CNTs. Most remarkably, they exhibit higher thermal stability, higher resistance to oxidation, and outstanding chemical stability.[2,3] These characteristics are particularly useful in devices subjected to hazardous and high temperature environments, where CNTs cannot be employed. Biomedical applications of water-dispersible BNNTs are envisaged as well in the areas of targeted drug delivery,[4] boron neutron capture therapy,[5] and electroporation therapy.[6] For optimal performance, BNNTs must be dispersed as isolated entities throughout a solid or fluid matrix. However, strong dispersion interactions between nanotubes lead to the spontaneous formation of bundles that clump together into larger aggregates.[7] This tendency is particularly strong in the case of BNNTs as a consequence of the polarity of the B−N bond, which leads to more complicated intertube interactions and significantly hinders BNNT purification, dispersion, and chemical modification. Initial attempts to functionalize BNNTs were inspired by chemical approaches originally developed for CNTs. For instance, inherent BNNTs' amino groups or hydroxides (approximately 3−15 at.% N[8,9]) were used as handles for the covalent attachment of acyl chlorides[10] or isocyanates.[11] The amount of amino or hydroxyl groups on the BNNTs was increased by plasma treatment[9,12,13] and by reaction with H_2O_2[8] or concentrated nitric acid[14] at high temperature and/or pressure. Such harsh conditions often lead to noticeable changes in the morphological and electronic properties of the BNNTs.[15]

Received: July 24, 2013
Revised: August 29, 2013
Published: August 29, 2013

dx.doi.org/10.1021/jp4073729 | J. Phys. Chem. C 2013, 117, 19568−19576

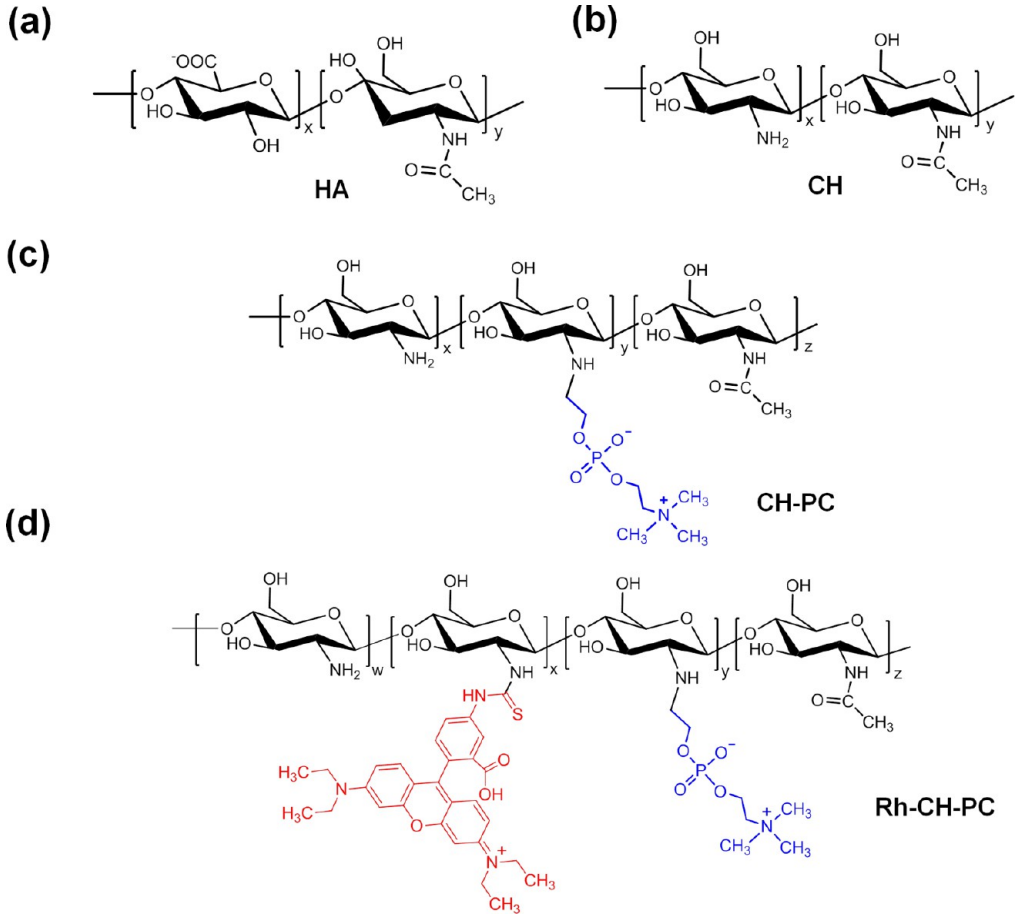

Figure 1. Chemical structures of (a) hyaluronic acid (HA), (b) chitosan (CH), (c) chitosan phosphorylcholine (CH-PC), and (d) rhodamine-B-labeled chitosan phosphorylcholine (Rh-CH-PC).

Water-borne BNNT hybrids were obtained by further treatment of BNNTs with hydrophilic polymers including polyelectrolytes, such as polynucleotides,[16] proteins,[17] peptides,[18] polyethyleneimine,[19] poly(L-lysine),[20] and glycol-chitosan,[21] and neutral polymers, such as poly(ethylene glycol) (PEG)[22−24] and glycodendrimers.[25] In most cases, however, coated BNNTs often present extensive sections of bare sidewalls, rarely exhibiting uniform core−shell morphology. Examination of reported transmission or scanning electron micrographs (TEM or SEM) of hydrophilic BNNT hybrids reveals also that individually coated BNNTs often coexist in suspension with coated bundles of BNNTs. These shortcomings greatly limit the usefulness of water-borne BNNT hybrids in biotechnological applications, such as nanosensors, and in nanomedicine where nonbiofouling well-defined materials are necessary.

The intrinsic polarity of the B−N bond offers access to precisely crafted functionalization chemistries performed with high yield under mild conditions. Hence amines interact with boron atoms of the BNNT sidewall via charge transfer interactions, yielding hybrid BNNTs stable in dispersions without modification of the tube electronic properties.[22] Several research groups have computed the adsorption energy of various amines onto BNNTs,[26−29] including ammonia, glucosamine, several amino acids, and nucleobases. In the case of glycine (NH_2-CH_2-COOH) the exothermic adsorption energy was calculated to be 0.34 eV.[26] Density functional theory calculations indicate that glycine can be chemically adsorbed on the BNNT sidewall and covalently bonded with the boron atom to form a B−N bond with a length of 1.74−1.77 Å.[26]

Inspired by these theoretical investigations, we set about to assess experimentally the interactions of BNNTs with glycine. We discovered that this simple amino acid is remarkably efficient in breaking up pristine BNNT bundles, yielding hydrophilic BNNTs dispersed in water as individual, debundled, nanotubes. Moreover, polyelectrolytes readily adsorbed onto individual glycine-modified BNNTs (Gly-BNNTs), as demonstrated here in the case of three polysaccharides, hyaluronic acid (HA), chitosan (CH), and a chitosan derivative bearing phosphorylcholine groups (CH-PC), widely used as drug-delivery vehicles, scaffolds for tissue engineering, and as biomaterials components:[30−34] (Figure 1). Hyaluronic acid is distributed widely within connective, epithelial, and neural tissues where it plays important biological functions. It is produced commercially by bacterial fermentation and has found numerous applications in drug delivery systems, synovial fluid replacement therapies, in neutraceuticals, and cosmetics formulations.[32,33] Chitosan is a linear polycation, composed of β-D-glucosamine and β-D-N-acetylglucosamine residues in (1→4) linkage. It is derived from chitin, a polymer extracted from the exoskeleton of numerous arthropods.[30] It is under consideration for several biomedical applications, such as matrices for tissue engineering and gene therapy formulations. CH-PC is a derivative of chitosan, which unlike chitosan, is readily soluble under physiological conditions by virtue of the

dx.doi.org/10.1021/jp4073729 | J. Phys. Chem. C 2013, 117, 19568−19576

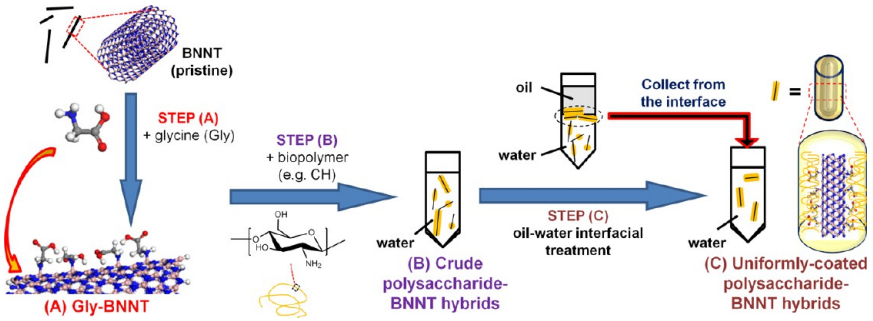

Figure 2. The schematic of the fabrication of the polysaccharide-BNNT hybrids. See Figure S1 in the Supporting Information for the experimental details.

PC substituents,[35] and consequently, more amenable to applications in biology and nanomedicine, such as the immunoisolation of red blood cells.[36] The polymers selected differed not only in structure and charge but also in molecular weight (see Experimental Section). This choice was intentional, since we wanted to test the versatility of the process. Considering the potentials of hybrid BNNTs in bionanotechnology, the simple, general, and mild method to produce robust hydrophilic BNNTs uniformly coated with biopolymers, described in this report, is a significant advance toward biomedical applications of BNNTs.

EXPERIMENTAL METHODS

Materials. Chitosan (CH, Figure 1a) with 75−85% deacetylation degree and a viscosity of 5−20 mPa·s (0.5% in 0.5% acetic acid solution at 20 °C) was purchased from TCI (Japan). High-molecular-weight hyaluronic acid (HA, Figure 1b) produced by microbial fermentation (about 2 MDa) was a gift from Soliance (France). The polymers were used as received. Chitosan (50−100 kDa) covalently grafted with 20% mol phosphorylcholine (CH-PC, Figure 1c) with respect to glucosamine residues was prepared as described previously.[35] Rhodamine-B isothiocyanate was obtained from Sigma-Aldrich. All other chemicals were received from Wako (Japan). Rhodamine-B labeled CH-PC (Rh-CH-PC) was prepared following known procedures (see Supporting Information, Section A). Ultrapure Milli-Q water (18.2 MΩ·cm, Millipore water purifier) was used for the preparation of all the solutions and suspensions. High-purity multiwalled BNNTs were synthesized by boron oxide-assisted chemical vapor deposition (BOCVD) as reported previously.[2]

Fabrication of BNNT/Polymer Hybrid Nanotubes. A schematic illustration of each step of the fabrication is shown in Figure S1, Supporting Information.

Preparation of Gly-BNNTs. A dispersion of pristine BNNT aggregates (0.85 mg) in ethanol (850 μL) was sonicated in a water bath (38 kHz, 60W, 15 min) in order to reduce the size of BNNTs aggregates. The BNNTs were isolated by centrifugation and dried under vacuum (<10 Pa) at room temperature. The dried BNNTs were redispersed in an aqueous glycine solution (1 M, 850 μL). The dispersion was sonicated for 30 min at room temperature, yielding a stable dispersion of Gly-BNNTs in water.

Preparation of Polymer-Coated BNNTs. Stock solutions of CH, CH-PC, and Rh-CH-PC (1 mg/mL) were prepared by dissolving the polymers in 0.2 M aqueous acetic acid. The HA solution (1 mg/mL) was prepared in deionized water. A polymer solution (1 mg/mL, 200 μL) was added in one shot to the Gly-BNNT aqueous suspension. Following a 5-min sonication, a turbid suspension was obtained. It was shaken overnight on a benchtop vortexer (1,000 rpm, room temperature). The crude polymer-coated BNNTs were separated by centrifugation and washed twice with deionized water (15,000 rpm, 5 min, 10 °C) in order to remove excess glycine and polymers. The purified hybrid BNNTs were resuspended in water (850 μL). An aliquot of the dispersion (200 μL) was placed in a 2-mL flask, followed by hexane (400 μL). The mixture was sonicated for 5 min and kept still at room temperature. A film of hybrid BNNTs formed gradually at the hexane-water interface. The segregated film was collected by pipetting in turn, first, the lower aqueous phase and, second, the hexane phase. The film was dried under vacuum to give a uniformly polymer-coated hybrid BNNTs, which readily redispersed in Milli-Q water after a few seconds sonication.

Characterizations. Samples for transmission or scanning electron microscopy (TEM or SEM) were prepared by deposition of an aliquot of a hybrid BNNTs suspension in water either on a native silicon wafer or on a 200-mesh collodion-coated copper grid (Nisshin EM, Japan) for field emission SEM (Hitachi SU8000, 5 kV) and TEM (Jeol JEM-3000F, 300 kV) observations, respectively. Electron energy-loss spectroscopy (EELS) was performed on selected regions of samples observed with a (Jeol JEM-2100F, 200 kV) TEM using a Gatan 766 spectrometer (Enfina 1000). The beam spot size was 0.7 nm. The regions were scanned with spatial drift correction at a dwell time of 1.5 s per pixel and a pixel size of about 5 nm. Optical micrographs were acquired in either dark field or bright field in the reflection mode with a Nikon Eclipse ME600L optical microscope mounting a halogen light source and a digital camera (DXM1200, Nikon) which can deliver up to 12 megapixel (3840 × 3072)-resolution photographs. Samples for X-ray photoelectron spectroscopy (XPS) were prepared by drop-casting a concentrated suspension of the crude or purified polymer-coated hybrid BNNTs (~10 mg/mL) on a native silicon wafer. Photoelectron spectra of the resulting films were acquired on a Theta Probe spectrometer (Thermo Fisher Scientific, Inc., Waltham, MA, USA) using a monochromatic Al Kα X-ray probe (1486.6 eV) under an ultrahigh vacuum of 2×10^{-6} Pa. The spot size of the incident beam, operated at 15 kV (6 mA), was 400 μm. A low-energy flood gun was employed for charge compensation. A pass energy of 30 eV, a step size of 0.1 eV, and a dwell time of 200 ms were used for narrow scans. In the standard mode of operation, photoelectrons over the range 20° to 80° with respect to the sample normal were collected. All core-level spectra were referenced to the C1s hydrocarbon peak (C−C/

dx.doi.org/10.1021/jp4073729 | J. Phys. Chem. C 2013, 117, 19568−19576

C−H) at 285.0 eV.[37] The spectrometer is also capable of simultaneous collection of photoelectron signals from various takeoff angles in the angle-resolving mode of operation. To obtain the surface chemical composition at different sampling depths, 12 takeoff angles from 12.5 to 67.5° were analyzed. Thermogravimetric analysis (TGA) was performed on a SII Exstar 6300 thermogravimetric/differential thermal instrument (Seiko, Japan). Specimens were heated at a rate of 10 °C·min^{-1} from room temperature to 650 °C in a platinum pan under a nitrogen stream (flow rate: 200 cm^3·min^{-1}). Alumina was used as reference. The samples were kept in vacuum (<10 Pa) before the TGA measurement.

Diffuse reflectance infrared Fourier transform (DRIFT) spectroscopy (DRIFT) was performed on a Thermo Nicolet 4700 Fourier transform infrared (FTIR) spectrometer equipped with a diffuse reflectance Smart Collector accessory. About 0.2 mg of a dried specimen, obtained by freeze-drying from an aqueous suspension, was dispersed in 350 mg of finely ground KBr powders. The resolution was set at 4 cm^{-1}. A total of 128 scans were acquired.

RESULTS AND DISCUSSION

Uniformly coated polysaccharide-BNNT hybrids were obtained by adsorption of a polymer on preformed glycine-modified BNNTs (Gly-BNNT). A subsequent oil/water interfacial treatment was needed to achieve a high yield of uniformly coated core−shell BNNT hybrids, as depicted in Figure 2, and described in the following sections.

Gly-BNNTs. Addition of a glycine solution to pristine BNNTs with the aid of mild sonication yielded a milky sol stable for a few hours after sonication. With time, the Gly-BNNTs settled by gravity, but they readily redispersed in water via vortexing or short-duration sonication. This behavior is quite different from that observed for dispersions of pristine BNNTs in common organic solvents, such as ethanol, acetone, dimethylformamide, and tetrahydrofuran, where agglomeration of BNNTs occurs almost instantaneously after discontinuation of the sonication. The exceptional stability of Gly-BNNTs is attributed to the electrostatic stabilization provided by the carboxylate groups of the adsorbed glycine. The successful functionalization of pristine BNNTs was supported by TEM observation, which indicated that Gly-BNNTs are coated along their longitudinal axis with a uniform 4−5 nm thin layer of glycine (see Figure S2, Supporting Information).

Polysaccharide-BNNT Hybrids. Aqueous suspensions of preformed Gly-BNNT supplemented with polysaccharides remained colloidally stable for extended periods of time (up to 48 h), especially in the cases of CH-PC and CH, where electrostatic attraction between the glycine carboxylates and the polymer amine groups are expected to strengthen the polymer/BNNT sidewall interaction. The sample treated with hyaluronic acid (HA-BNNT) showed a tendency toward sedimentation upon standing at room temperature. The poorer stability of the HA-BNNT suspension, compared to CH-BNNT and CH-PC-BNNT, can be attributed to the absence of favorable electrostatic interactions between HA and Gly-BNNT and to the higher molecular weight of HA (2 MDa vs. 100 kDa for CH and CH-PC).[38] In a control experiment, polysaccharides were added to dispersions of pristine BNNTs (in the absence of Gly). The dispersions settled immediately when kept still, highlighting the critical role of glycine in facilitating the formation of stable BNNT/polysaccharide hybrids.

Dark field optical micrographs of several hybrid BNNTs are presented in Figure 3 (b to d). Under dark field illumination,

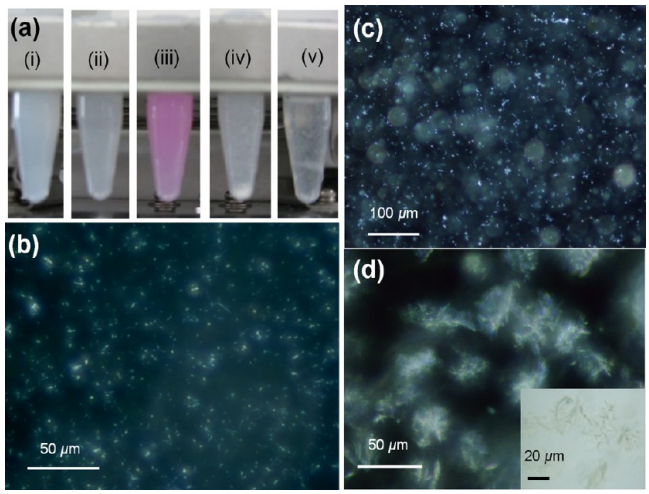

Figure 3. (a) Photograph of BNNT dispersions in aqueous glycine solutions (1 M), *prior to* the liquid−liquid interfacial treatment, that contain (i) CH, (ii) CH-PC, (iii) Rh-CH-PC, (iv) HA, and (v) no polymer. Dark field optical micrographs of aqueous dispersions of crude CH-PC-BNNTs (b) before centrifugation and (c) after centrifugation and redispersion of the pellet in water. (d) Dark field optical micrograph of a dispersion in water of CH-PC BNNTs prepared by coating pristine BNNTs *without pretreatment with glycine* (step A in Figure 2). Inset: bright field optical image corresponding to (d).

only the light beams scattered at oblique angles illuminate the sample. The dispersed light from the light source does not hit the sample. Hence, the image is formed exclusively from higher-order diffraction beams scattered by the specimen. Any nonscattered or nondiffracted light is excluded from the image causing the background to appear black. Therefore dark field microscopy is a very sensitive tool to distinguish nonabsorbing specimens even if their refractive index is only slightly different from that of the surrounding medium. It allows one to observe readily surface features of the BNNT edges, where refractive index gradients occur. Both reflection and refraction events produce relatively small angular changes of the oblique light, allowing some light to enter the objective. Due to the strong scattering of light from the suspending micrometer-long BNNTs, each BNNT appears as a glowing spot. In order to minimize diffraction artifacts from the out-of-focus light that obscures the specimen details, the BNNT suspension deposited on the silicon wafer was carefully spread to form a uniform thin aqueous layer over the entire wafer surface. The micrographs shown in Figure 3b and 3c correspond to CH-PC suspensions before and after purification by centrifugation. The overall appearance of the two samples is the same: they present distinct bright spots, attributed to the BNNTs, surrounded by a diffuse halo indicative of the presence of hydrated polymer chains. The bright spots are distributed evenly throughout the micrograph. In contrast, the micrograph (Figure 3d), which corresponds to a suspension of CH-PC and pristine BNNTs, predominantly features large clusters of BNNTs (>10 μm in size) surrounded by a diffuse bright cloud, attributed to CH-PC chains coated onto BNNT agglomerates. The inset in Figure 3d presents a micrograph

dx.doi.org/10.1021/jp4073729 | J. Phys. Chem. C 2013, 117, 19568−19576

of the same sample observed under normal conditions. BNNT clusters are clearly observed.

CH-PC-BNNTs hybrids were also observed by SEM (Figure 4). The samples feature mostly isolated nanotubes with very

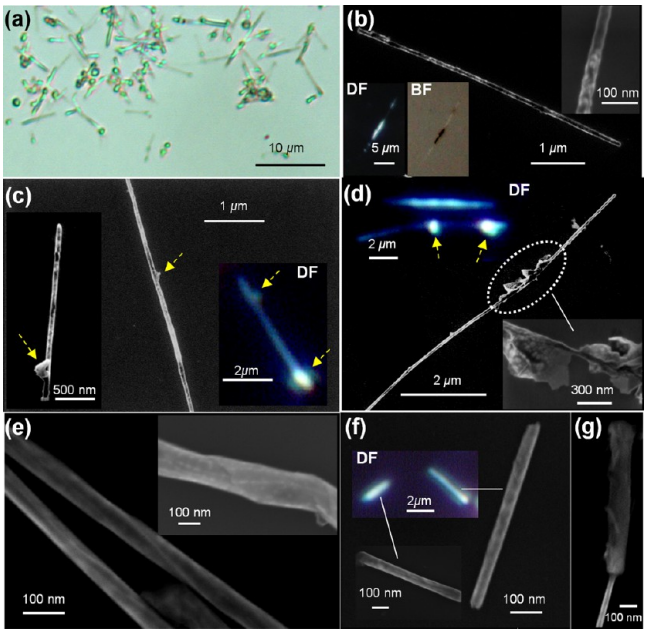

Figure 4. (a) Optical micrograph of an ensemble of crude CH-PC-BNNTs *prior to* interfacial treatment. (b) SEM and optical images of a BNNT partially coated with CH-PC (insets: DF and BF denote a dark field and bright field micrograph, respectively). (c)-(d) SEM and optical images of some BNNTs with unevenly distributed CH-PC coating along their longitudinal direction (the arrows highlight locations of excessive, loosely bound polymer). (e)-(f) SEM and optical images of CH-PC-BNNTs uniformly coated along their longitudinal direction. (g) SEM image of a discrete CH-PC-BNNT in which both thin and thick polymer layers coexist on the same nanotube.

few aggregates and bundles (Figure 4a). The surface morphology of the nanotubes varies greatly throughout the sample. In some cases, the coating is not uniform at all, as shown in Figure 4b, that depicts an individual CH-PC-BNNT very poorly coated. Polymer patches, sparsely adsorbed to the sidewalls of the BNNTs, leave large sections of bare BNNTs. Contrast enhancement by dark field imaging, compared to bright field imaging, emphasizes the patchiness of the coating (see insets in Figure 4b). Other examples of unevenly coated BNNTs are illustrated in Figure 4c and 4d. Within the ensemble of CH-PC-BNNTs, we also observed evenly coated BNNTs, but they were the minority components (on the order of ~20% as qualitatively estimated from the SEM images). Examples of uniformly coated CH-PC-BNNTs are shown in Figures 4e to 4g. The inset in Figure 3e is a high-resolution SEM image highlighting a section of a long individual BNNT that was uniformly coated with a thick CH-PC layer. The overall external diameter of this nanotube, including the polymer wrapping, is about 150 nm, a value much larger than the average diameter of pristine BNNT (~ 50 nm). Figure 4g displays an example of a CH-PC-BNNT for which some sections are coated with a thin polymer layer, while other sections are covered with a very thick layer. Under dark-field microscopy observation, uniformly coated BNNTs emerge as lasing rods, as shown in the inset image of Figure 4f. A study of BNNT hybrids obtained with CH and HA also revealed a wide disparity of nanotube coverage within a given sample, pointing to the necessity to carry out further treatment of the suspensions in order to extract, and possibly amplify, the fraction of evenly coated BNNTs from the crude mixture.

As stated in the Introduction, for biomedical applications, it is highly desirable to use BNNTs coated throughout their longitudinal direction. Therefore, we set out to isolate fully coated BNNT hybrids from the crude mixtures obtained initially. Standard techniques, such as successive centrifugations using different speeds,[39,40] were not effective. In contrast, an oil/water interfacial treatment, known to promote the assembly of nanomaterials into higher-order structures,[41] proved to be surprisingly effective and very simple. A layer of hexane (the oil) was placed on top of an aqueous suspension of a crude polymer-coated BNNT mixture. The two-phase system was subjected to sonication. Oily flocs were generated in the aqueous phase eventually yielding a uniform emulsion. The emulsion was not stable under static conditions: larger flocs formed gradually and migrated toward the hexane phase. They finally formed a segregated film on the oil−water interface. Dark and bright field optical micrographs of the segregated film recovered immediately after sequential removal of the bottom aqueous layer, and the top hexane layer are presented in Figure S1 (Supporting Information). Surprisingly, the film consists of clustered liquid droplets, >15 μm in diameter, that resist coalescence upon standing. Further air drying yielded a solid film that readily disintegrated in water to form a stable suspension.

By analogy with the known property of CNTs[42] and cellulose nanocrystals[43] to act as emulsion Pickering agents, we suggest that the liquid droplets formed in the emulsification process are stabilized by BNNTs adsorbed to the oil/water interface. During sonication, numerous oil droplets were generated in the aqueous phase; polymer-coated BNNTs adsorbed onto the oil/water interface in order to reduce the surface tension of the oil droplets. The surface tension of individual pristine BNNTs (with a diameter of 40 nm) is on the order of 20−30 mN/m,[44] a value close to that of hexane (18.4 mN/m[45]). The surface tension of aqueous CH[46] and HA[47] solutions is lower than that of water. Thus, polysaccharides adsorbed on BNNTs tend to reduce the interfacial tension between water and the hexane droplets, such that polysaccharide-coated BNNTs act as weak emulsifiers. Structural reorganization of the polymer coating toward a uniform distribution of the polymer over the entire BNNT surface is expected to occur in order to minimize the hexane-water interfacial tension during the two-phase purification. Analyses by SEM and TEM described in the following sections confirmed that surface reorganization of the polymer coating indeed occurred.

We examined by SEM the morphology of the layer recovered from the water/hexane interface at the end of the process depicted in Figure 2, section C, as well as the morphology of the BNNTs recovered upon redispersion of the film in water. Micrographs of films and dispersions are presented in Figure 5 (a,b) and 5 (c,d), respectively, in the case of CH-PC-BNNT hybrids. It is striking to observe that most BNNTs, if not all, are totally covered with polymer. The polymer coat has a multilayered, sheath-like morphology, as seen in the inset of Figure 5b, which presents a cross-section of a BNNT tube end. The arrow points to the hollow cavity of the tube, which is surrounded by a polymer layer wrapped coaxially around the nanotube, such that the CH-PC-BNNTs adopt a core−shell

dx.doi.org/10.1021/jp4073729 | J. Phys. Chem. C 2013, 117, 19568−19576

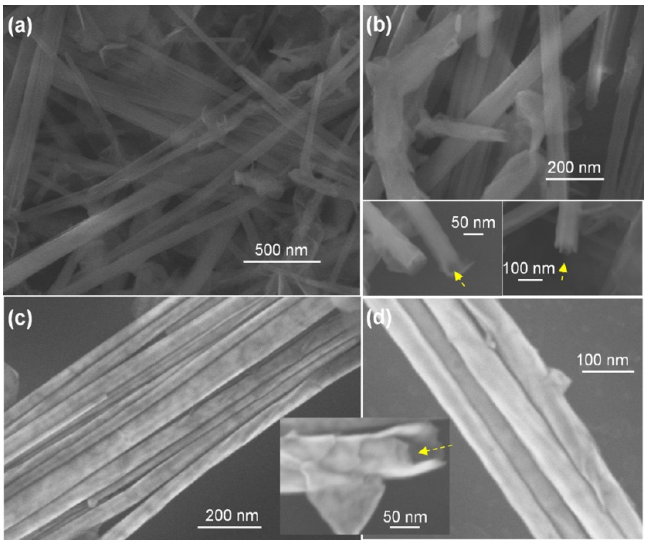

Figure 5. (a) SEM micrograph of the film of the CH-PC-BNNTs collected from the hexane-water interface after the liquid–liquid interfacial treatment and vacuum-dried on a silicon wafer. Morphological details, including the body and the tip of the nanohybrids are shown under higher higher-magnification in (b). (c)-(d) SEM images of an ensemble of the CH-PC-BNNTs deposited on a silicon wafer from a dilute suspension in water (inset: high-resolution SEM image of the cracked tip of a CH-PC-BNNT which exhibits the multilayered structure of the thick polymer 'skin' on the exterior of a BNNT). The arrows point to the cross-sectional faces of the nanohybrids, where the lumens are revealed.

morphology. This uniform morphology facilitates the formation of organized nanotube assemblies, such as the long bundles of CH-PC nanotubes seen in Figures 5c and 5d (also Supporting Information, Figure S3b and S3c for HA-BNNTs). The formation of higher order structures is promoted by the evaporation of water during the preparation of the SEM specimen of a dilute dispersion of CH-BNNTs deposited on a silicon wafer. The film prior to resuspension in water consists of a web of intercalated CH-PC-BNNTs oriented at random (Figures 5a and 5b).

The presence of a polymer layer around BNNTs was confirmed by high-resolution TEM (HRTEM) coupled with electron energy loss spectroscopy (EELS). HRTEM images of purified BNNT hybrids formed with CH, CH-PC, and rhodamine-B-labeled CH-PC (Rh-CH-PC) are presented in Figure 6 (a, b, c). The diameter of the BNNT core of the hybrids is indicated by the red arrows. The thickness of the polymer layer is ~10 nm. A low magnification TEM micrograph of CH-PC-BNNT is shown as an inset in Figure 6b. The nanotube shown is uniformly coated along its entire length. Elemental analysis of the outer layer of the BNNTs unambiguously confirmed that this layer can be attributed to a carbon-rich polymer film. Two strong core-loss edge peaks present in the EEL spectra were particularly useful: the peak peculiar for the C K edge was attributed to the polymer film, and the peak natural for the B K edge was ascribed to the BNNT. The N K edge peak cannot be used since signals due to the polymer and to BNNT overlap. EEL spectra of two individual CH-PC-coated nanotubes are given in Figure 6d. The thickness of the polymer layer wrapping the BNNT is different for the two samples. The lumen of the sample S1 (left) is more transparent to electrons (thinner polymer coating) than that of S2. Correspondingly, the intensity of the C K core loss edge peak, relative to the B K core loss edge

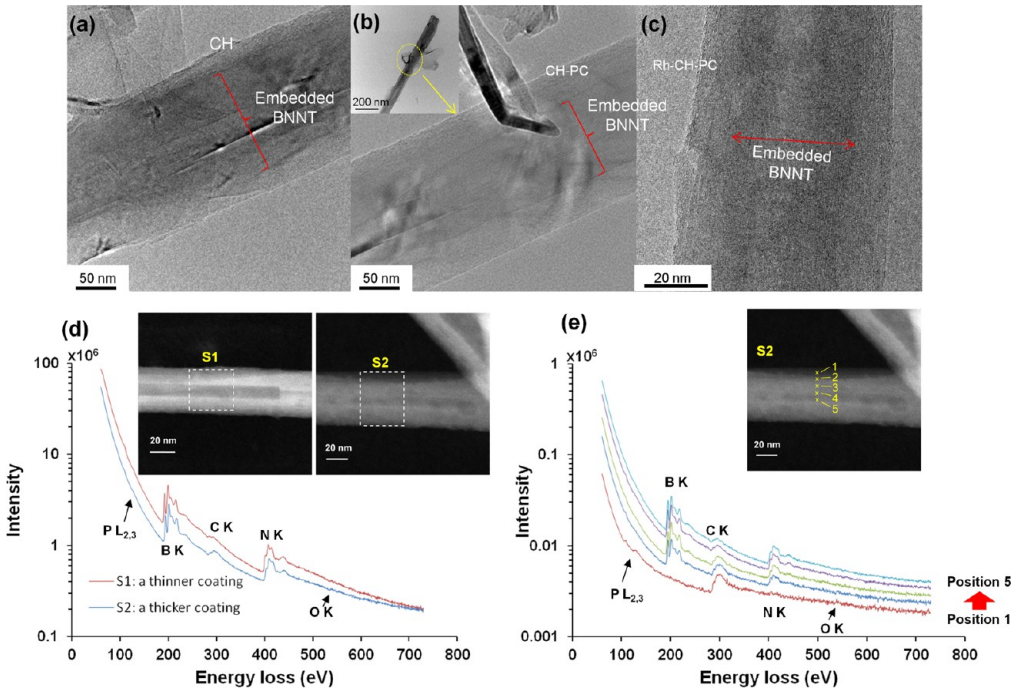

Figure 6. (a) High-resolution TEM images of a section of individual NTs (a) CH-BNNT, (b) CH-PC-BNNT, and (c) Rh-CH-PC-BNNT obtained after the liquid–liquid interfacial treatment (inset: a low-magnification TEM image of a CH-PC-BNNT demonstrating the uniform distribution of the polymer layer along the longitudinal axis of the nanotube). (d) Summed EEL spectra recorded for the tube regions within the rectangular areas S1 and S2 of two individual CH-PC-BNNTs coated with a thin polymer layer (S1) and a thicker polymer layer (S2). (e) Spatially resolved EEL line profiles of the CH-PC-BNNTs S2 recorded in the axial direction from the exterior (position 1) to the center (position 5) of the nanotube.

dx.doi.org/10.1021/jp4073729 | J. Phys. Chem. C 2013, 117, 19568–19576

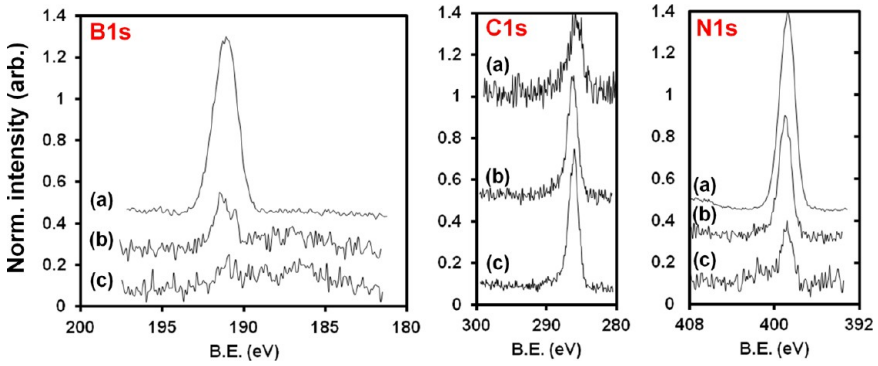

Figure 7. Standard high-resolution XPS B1s, C1s, and N1s elemental scans of (a) pristine BNNTs, (b) crude CH-PC-BNNTs prior to the liquid–liquid interfacial treatment (i.e., state B in Figure 2), and (c) purified CH-PC-BNNTs obtained after the liquid–liquid interfacial treatment (i.e., the state C in Figure 2).

peak, is weaker in the EEL spectrum of S1, compared to S2. EEL spectra of the sample S2 recorded for various positions along the radial direction of the tube are presented in Figure 6e. The spectrum corresponding to position 1 (outermost region from the sidewall) features a strong C K edge peak; the B K edge peak cannot be distinguished from the background of this spectrum. Moreover, this spectrum presents a P $L_{2,3}$ edge peak attributed to the phosphorus of the phosphorylcholine substituents of CH-PC, giving strong evidence that the exterior layer indeed contains polymer chains. In spectra acquired at positions closer to the tube lumen, the intensity of the B K edge peak increases as the position moves toward the lumen, while the C K edge peak decreases in intensity.

The chemical composition of the surface of BNNT hybrids was determined by XPS analysis, which reports the overall composition over a depth of ~10 nm. Core energy level spectra of pristine BNNTs (spectra a), CH-PC-BNNT prior to interfacial treatment (step B in Figure 2, spectra b), and CH-PC-BNNT isolated after interfacial treatment (step C in Figure 2, spectra c) are presented in Figure 7 for the core levels B1s, C1s, and N1s. The XPS spectrum of pristine BNNTs (spectrum a) exhibits characteristic signals at ~191 eV and ~399 eV attributed to the B1s and N 1s energy levels, respectively. The weak signal centered at ~285.5 eV, attributed to C1s, suggests the presence of hydrocarbon contaminants on the BNNT surface. The C1s signal is much stronger in the spectrum b recorded for CH-PC-BNNT sample prior to interfacial purification, vouching for the presence of a polymer layer on this sample. Spectrum b also displays a weak B1s signal reflecting the presence of bare BNNT sections as observed on SEM micrographs (Figure 4b). This signal is absent in spectrum c, acquired for a CH-PC-BNNT sample that has undergone the interfacial treatment. This observation strongly confirms the successful coverage of the overall BNNT surface by a ~10 nm-thick polymer layer verified also by SEM and TEM. The detailed features of the N1s signal in spectrum c also are characteristics of the CH-PC outer layer and not of the BNNT core. The shoulders at 401–403 eV can be ascribed to charged N species of CH-PC.[48] Angle resolved XPS analysis of a CH-PC-BNNT sample post-treated as a function of takeoff angles (12.5 to 67.5°), a range that corresponds to a sampling depth of 2.3 to 9.8 nm,[48] failed to detect signals due to B1s, whereas C–C/C–H, C–O, and C–N C1s atoms were readily observed (see Figure S6). XPS analysis of a sample of CH-PC-Rh-BNNT post-treated revealed a weak signal (291–293 eV) attributed to the $\pi \rightarrow \pi^*$ shakeup satellite characteristic of the aromatic groups in the rhodamine-B structure (Figure S7a).

Bulk characterization of the BNNT hybrids was performed as well. Thermogravimetric analysis revealed that the thermal stability of the polymers increased upon adsorption onto BNNTs, as observed in previous studies.[49] This was particularly apparent in the case of HA, for which the main decomposition transition temperature increased from 240 to 350 °C (see Figure S4b, Supporting Information). Diffuse reflectance infrared Fourier transform (DRIFT) measurements on hybrid BNNTs, isolated as powders after the interfacial treatment, confirmed the presence of polysaccharides (see Figure S5, Supporting Information). Two absorption bands (indicated with dotted arrows) are particularly useful: (i) the band between 2900 and 2750 cm^{-1}, assigned to the aliphatic C–H stretching vibrations; and (ii) the band around 3500–3600 cm^{-1}, ascribed to the N–H/O–H stretching vibrations. These bands are absent in the DRIFT spectrum of pristine BNNTs. On the contrary, the two bands[49] around 1370 and 818 cm^{-1} (indicated with asterisks), which are characteristic of pristine BNNTs appear as strong bands in the DRIFT spectrum of the BNNT nanohybrids. Hence, as expected, the DRIFT spectrum of BNNT hybrids (here CH-PC-BNNT) carries the signature of both CH-PC and BNNT.

■ CONCLUSIONS

For applications in bionanotechnology, such as supporting matrices for tissue engineering or as drug delivery vehicles, it is of paramount importance to use uniformly biopolymer-coated BNNTs in order to preclude possible deleterious effects, such as cytotoxicity or biofouling. We reported here a mild and efficient method to obtain polysaccharide-coated BNNTs that present the desired core/shell morphology. This was achieved by using two steps that were never used in the processing of BNNTs: (a) pretreatment with glycine and (b) liquid–liquid interfacial treatment to amplify the coverage of the tube and separate fully coated BNNTs from the imperfect ones. This work has relevant practical implication in improving the biocompatibility and the dispersion of BNNTs. Also, it exhibits inherent "green-ness" as all steps of the process are performed at room temperature under mild conditions without the need for strong acids, alkali, or oxidants. This achievement is of marked importance, when processing BNNTs targeted for therapeutic applications, since the BNNT cargo, drugs, proteins, or gene vectors easily denature and are deactivated upon heating. Moreover any residual acidic or oxidative

dx.doi.org/10.1021/jp4073729 | J. Phys. Chem. C 2013, 117, 19568–19576

compounds may leach slowly from the hybrids and cause undesired cytotoxic effects. Work in progress indicates that the BNNT hybrids described are readily modified with bioactive compounds, opening the way to novel biodevices that take advantage of the intrinsic properties of BNNTs and their biocoating.

■ ASSOCIATED CONTENT

Supporting Information

Additional information on (A) the synthesis of the Rh-CH-PC polymer, (B) the schematic of each step of the fabrication of the polysaccharide-BNNT hybrid, (C) TEM and XPS characterization of Gly-BNNTs, (D) the SEM examination of uniformly coated HA-BNNT hybrids, (E) the TGA data, (F) the DRIFT data, (G) the angle-resolved XPS data, and (H) the fluorescence measurement. This material is available free of charge via the Internet at http://pubs.acs.org.

■ AUTHOR INFORMATION

Corresponding Authors

*Phone: +81-29-860-4432. E-mail: golberg.dmitri@nims.go.jp (D.G.).

*Phone: +1-514-340-5179. E-mail: francoise.winnik@umontreal.ca (F.M.W.).

Notes

The authors declare no competing financial interest.

■ ACKNOWLEDGMENTS

We thank K. Tashiro and I. Yamada of the National Institute for Materials Science (NIMS) for offering technical assistance in using the fluorescence spectrometer and TEM-EELS, respectively, for characterizing our BNNT samples. We also thank T. Sato from the Department of Macromolecular Science of Osaka University for fruitful discussions on this paper.

■ REFERENCES

(1) See for instance: Interfacial Nanoarchitectonics Special Issue, *Langmuir* **2013**, *29*, issue 24. Special Issue: WPI Research Center for Materials Nanoarchitectonics, NIMS, *Adv. Mater.* **2012**, *24*, issue 2.

(2) Golberg, D.; Bando, Y.; Huang, Y.; Terao, T.; Mitome, M.; Tang, C. C.; Zhi, C. Y. Boron Nitride Nanotubes and Nanosheets. *ACS Nano* **2010**, *4*, 2979−2993.

(3) Wang, J. S.; Lee, C. H.; Yap, Y. K. Recent Advancements in Boron Nitride Nanotubes. *Nanoscale* **2010**, *2*, 2028−2034.

(4) Ciofani, G. Potential Applications of Boron Nitride Nanotubes as Drug Delivery Systems. *Expert Opin. Drug Delivery* **2010**, *7*, 889−893.

(5) Ciofani, G.; Raffa, V.; Menciassi, A.; Cuschieri, A. Folate Functionalized Boron Nitride Nanotubes and their Selective Uptake by Glioblastoma Multiforme Cells: Implications for their Use as Boron Carriers in Clinical Boron Neutron Capture Therapy. *Nanoscale Res. Lett.* **2009**, *4*, 113−121.

(6) Raffa, V.; Riggio, C.; Smith, M. W.; Jordan, K. C.; Cao, W.; Cuschieri, A. BNNT-Mediated Irreversible Electroporation: its Potential on Cancer Cells. *Technol. Cancer Res. Treat.* **2012**, *11*, 459−465.

(7) Hao, S. G.; Zhou, G.; Duan, W. H.; Wu, J.; Gu, B.-L. Transverse Pressure Induced Phase Transitions in Boron Nitride Nanotube Bundles and the Lightest Boron Nitride Crystal. *J. Am. Chem. Soc.* **2008**, *130*, 5257−5261.

(8) Zhi, C. Y.; Bando, Y.; Terao, T.; Tang, C. C.; Kuwahara, H.; Golberg, D. Chemically Activated Boron Nitride Nanotubes. *Chem. Asian J.* **2009**, *4*, 1536−1540.

(9) Sainsbury, T.; Ikuno, T.; Okawa, D.; Pacilé, D.; Frechét, J. M. J.; Zettl, A. Self-Assembly of Gold Nanoparticles at the Surface of Amine- and Thiol-Functionalized Boron Nitride Nanotubes. *J. Phys. Chem. C* **2007**, *111*, 12992−12999.

(10) Zhi, C. Y.; Bando, Y.; Tang, C. C.; Honda, S. H.; Sato, K.; Kuwahara, H.; Golberg, D. Covalent Functionalization Towards Soluble Multiwalled Boron Nitride Nanotubes. *Angew. Chem., Int. Ed.* **2005**, *44*, 7932−7935.

(11) Zhou, S.-J.; Ma, C.-Y.; Meng, Y.-Y.; Su, H.-F.; Zhu, Z.; Deng, S.-L.; Xie, S.-Y. Activation of Boron Nitride Nanotubes and their Polymer Composites for Improving Mechanical Performance. *Nanotechnology* **2012**, *23*, 055708.

(12) Ikuno, T.; Sainsbury, T.; Okawa, D.; Fréchet, J. M. J.; Zettl, A. Amine-Functionalized Boron Nitride Nanotubes. *Solid State Commun.* **2007**, *142*, 643−646.

(13) Dai, X. J. J.; Chen, Y.; Chen, Z. Q.; Lamb, P. R.; Li, L. H.; du Plessis, J.; McCulloch, D. G.; Wang, X. G. Controlled Surface Modification of Boron Nitride Nanotubes. *Nanotechnology* **2011**, *22*, 245301.

(14) Ciofani, G.; Genchi, G. G.; Liakos, I.; Athanassiou, A.; Dinucci, D.; Chiellini, F.; Mattoli, V. A Simple Approach to Covalent Functionalization of Boron Nitride Nanotubes. *J. Colloid Interface Sci.* **2012**, *374*, 308−314.

(15) Zhi, C. Y.; Bando, Y.; Tang, C. C.; Golberg, D. Engineering of Electronic Structure of Boron-Nitride Nanotubes by Covalent Functionalization. *Phys. Rev. B* **2006**, *74*, 153413.

(16) Zhi, C. Y.; Bando, Y.; Wang, W. L.; Tang, C. C.; Kuwahara, H.; Golberg, D. DNA-Mediated Assembly of Boron Nitride Nanotubes. *Chem. Asian J.* **2007**, *2*, 1581−1585.

(17) Zhi, C. Y.; Bando, Y.; Tang, C. C.; Golberg, D. Immobilization of Proteins on Boron Nitride Nanotubes. *J. Am. Chem. Soc.* **2005**, *127*, 17144−17145.

(18) Gao, Z. H.; Zhi, C. Y.; Bando, Y.; Golberg, D.; Serizawa, T. Isolation of Individual Boron Nitride Nanotubes via Peptide Wrapping. *J. Am. Chem. Soc.* **2010**, *132*, 4976−4977.

(19) Ciofani, G.; Raffa, V.; Yu, J.; Chen, Y.; Obata, Y.; Takeoka, S.; Menciassi, A.; Cuschieri, A. Boron Nitride Nanotubes: a Novel Vector for Targeted Magnetic Drug Delivery. *Curr. Nanosci.* **2009**, *5*, 33−38.

(20) Ciofani, G.; Ricotti, L.; Danti, S.; Moscato, S.; Nesti, C.; D'Alessandro, D.; Dinucci, D.; Chiellini, F.; Pietrabissa, A.; Petrini, M.; Menciassi, A. Investigation of Interactions between Poly-L-lysine-coated Boron Nitride Nanotubes and C2C12 Cells: Up-Take, Cytocompatibility, and Differentiation. *Int. J. Nanomed.* **2010**, *5*, 285−298.

(21) Ciofani, G.; Danti, S.; D'Alessandro, D.; Ricotti, L.; Moscato, S.; Bertoni, G.; Falqui, A.; Berrettini, S.; Petrini, M.; Mattoli, V.; Menciassi, A. Enhancement of Neurite Outgrowth in Neuronal-like Cells Following Boron Nitride Nanotube-Mediated Stimulation. *ACS Nano* **2010**, *4*, 6267−6277.

(22) Xie, S.-Y.; Wang, W.; Shiral Fernando, K. A.; Wang, X.; Lin, Y.; Sun, Y.-P. Solubilization of Boron Nitride Nanotubes. *Chem. Commun.* **2005**, 3670−3672.

(23) Lee, C. H.; Zhang, D. Y.; Yap, Y. K. Functionalization, Dispersion, and Cutting of Boron Nitride Nanotubes in Water. *J. Phys. Chem. C* **2012**, *116*, 1798−1804.

(24) Choi, J.-H.; Kim, J. W.; Seo, D. B.; Seo, Y.-S. Purification of Boron Nitride Nanotubes via Polymer Wrapping. *Mater. Res. Bull.* **2013**, *48*, 1197−1203.

(25) Chen, X.; Wu, P.; Rouseas, M.; Okawa, D.; Gartner, Z.; Zettl, A.; Bertozzi, C. R. Boron Nitride Nanotubes are Noncytotoxic and Can Be Functionalized for Interaction with Proteins and Cells. *J. Am. Chem. Soc.* **2009**, *131*, 890−891.

(26) Wu, X. J.; An, W.; Zeng, X. C. Chemical Functionalization of Boron-Nitride Nanotubes with NH_3 and Amino Functional Groups. *J. Am. Chem. Soc.* **2006**, *128*, 12001−12006.

(27) Rodríguez Juárez, A.; Chigo Anota, E.; Hernández Cocoletzi, H.; Flores Riveros, A. F. Adsorption of Chitosan on BN Nanotubes: a DFT Investigation. *Appl. Surf. Sci.* **2013**, *268*, 259−264.

(28) Mukhopadhyay, S.; Scheicher, R. H.; Pandey, R.; Karna, S. P. Sensitivity of Boron Nitride Nanotubes Toward Biomolecules of Different Polarities. *J. Phys. Chem. Lett.* **2011**, *2*, 2442−2447.

(29) Mukhopadhyay, S.; Gowtham, S.; Scheicher, R. H.; Pandey, R.; Karna, S. P. Theoretical Study of Physisorption of Nucleobases on Boron Nitride Nanotubes: a New Class of Hybrid Nano-Biomaterials. *Nanotechnology* **2010**, *21*, 165703.
(30) Dash, M.; Chiellini, F.; Ottenbrite, R. M.; Chiellini, E. Chitosan—A Versatile Semi-Synthetic Polymer in Biomedical Applications. *Prog. Polym. Sci.* **2011**, *36*, 981−1014.
(31) Yi, H. M.; Wu, L.-Q.; Bentley, W. E.; Ghodssi, R.; Rubloff, G. W.; Culver, J. N.; Payne, G. F. Biofabrication with Chitosan. *Biomacromolecules* **2005**, *6*, 2881−2894.
(32) Lapčík, L., Jr.; Lapčík, L.; De Smedt, S.; Demeester, J.; Chabreček, P. Hyaluronan: Preparation, Structure, Properties, and Applications. *Chem. Rev.* **1998**, *98*, 2663−2684.
(33) Murano, E.; Perin, D.; Khan, R.; Bergamin, M. Hyaluronan: From Biomimetic to Industrial Business Strategy. *Nat. Prod. Commun.* **2011**, *6*, 555−572.
(34) Tardif, K.; Cloutier, I.; Miao, Z. M.; Lemieux, C.; St-Denis, C.; Winnik, F. M.; Tanguay, J.-F. A Phosphorylcholine-Modified Chitosan Polymer as an Endothelial Progenitor Cell Supporting Matrix. *Biomaterials* **2011**, *32*, 5046−5055.
(35) Tiera, M. J.; Qiu, X. P.; Bechaouch, S.; Shi, Q.; Fernandes, J. C.; Winnik, F. M. Synthesis and Characterization of Phosphorylcholine-Substituted Chitosans Soluble in Physiological pH Conditions. *Biomacromolecules* **2006**, *7*, 3151−3156.
(36) Mansouri, S.; Merhi, Y.; Winnik, F. M.; Tabrizian, M. Investigation of Layer-by-Layer Assembly of Polyelectrolytes on Fully Functional Human Red Blood Cells in Suspension for Attenuated Immune Response. *Biomacromolecules* **2011**, *12*, 585−592.
(37) *Practical Surface Analysis by Auger and X-ray Photoelectron Spectroscopy*, 2nd ed.; Seah, M. P., Briggs, D., Eds.; Wiley: Chichester, U.K., 1992.
(38) Cosgrove, T. Polymers at Interfaces. In *Colloid Science: Principles, Methods and Applications*; Cosgrove, T., Ed.; Blackwell Publishing: Oxford, U.K., 2005; pp 113−142.
(39) Yu, A. P.; Bekyarova, E.; Itkis, M. E.; Fakhrutdinov, D.; Webster, R.; Haddon, R. C. Application of Centrifugation to the Large-Scale Purification of Electric Arc-Produced Single-Walled Carbon Nanotubes. *J. Am. Chem. Soc.* **2006**, *128*, 9902−9908.
(40) Sharma, V.; Park, K. W.; Srinivasarao, M. Shape Separation of Gold Nanorods using Centrifugation. *Proc. Natl. Acad. Sci. U.S.A.* **2009**, *106*, 4981−4985.
(41) Hu, L. F.; Chen, M.; Fang, X. S.; Wu, L. M. Oil-Water Interfacial Self-Assembly: a Novel Strategy for Nanofilm and Nanodevice Fabrication. *Chem. Soc. Rev.* **2012**, *41*, 1350−1362.
(42) Shen, M.; Resasco, D. E. Emulsions Stabilized by Carbon Nanotube-Silica Nanohybrids. *Langmuir* **2009**, *25*, 10843−10851.
(43) Capron, I.; Cathala, B. Surfactant-Free High Internal Phase Emulsions Stabilized by Cellulose Nanocrystals. *Biomacromolecules* **2013**, *14*, 291−296.
(44) Li, L. H.; Chen, Y.; Glushenkov, A. M. Boron Nitride Nanotube Films Grown from Boron Ink Painting. *J. Mater. Chem.* **2010**, *20*, 9679−9683.
(45) *CRC Handbook of Chemistry and Physics*, 77th ed.; Lide, D. R., Frederikse, H. P. R., Eds.; CRC Press: Boca Raton, FL, 1996.
(46) Geng, X. Y.; Kwon, O.-H.; Jang, J. H. Electrospinning of Chitosan Dissolved in Concentrated Acetic Acid Solution. *Biomaterials* **2005**, *26*, 5427−5432.
(47) Ribeiro, W.; Mata, J. L.; Saramago, B. Effect of Concentration and Temperature on Surface Tension of Sodium Hyaluronate Saline Solutions. *Langmuir* **2007**, *23*, 7014−7017.
(48) Miao, Z. M.; Kujawa, P.; Lau, Y. T. R.; Toita, S.; Qi, B. W.; Nakanishi, J.; Cloutier, I.; Tanguay, J. F.; Winnik, F. M. Tuning the Properties and Functions of 17β-Estradiol-Polysaccharide Conjugates in Thin Films: Impact of Sample History. *Biomacromolecules* **2012**, *13*, 4098−4108.
(49) Thakur, V. K.; Yan, J.; Lin, M.-F.; Zhi, C. Y.; Golberg, D.; Bando, Y.; Sim, R.; Lee, P. S. Novel Polymer Nanocomposites from Bioinspired Green Aqueous Functionalization of BNNTs. *Polym. Chem.* **2012**, *3*, 962−969.